1	Title
2	
3	Gene-regulatory independent functions for insect DNA methylation
4	
5	Short Title
6	
7	Functional DNA methylation in an insect
8	
9	Authors
10	
11	Adam J. Bewick <sup>1</sup> , Zachary Sanchez <sup>2</sup> , Elizabeth C. Mckinney <sup>2</sup> , Allen J. Moore <sup>2</sup> , Patricia
12	J. Moore <sup>2*</sup> , Robert J. Schmitz <sup>1*</sup>
13	
14	Affiliations
15	
16	<sup>1</sup> Department of Genetics, University of Georgia, Athens, GA 30602, USA
17	<sup>2</sup> Department of Entomology, University of Georgia, Athens, GA 30602, USA
18	
19	Corresponding Authors
20	

21 E-mail: \*pjmoore@uga.edu (PJM); \*schmitz@uga.edu (RJS)

## 22 Abstract

23

24 The function of cytosine (DNA) methylation in insects remains unknown. Here 25 we provide evidence for the functional role of the maintenance DNA methyltransferase 1 26 (Dnmt1) in an insect using experimental manipulation. Through RNA interference 27 (RNAi) we successfully post-transcriptionally knocked down *Dnmt1* in ovarian tissue of 28 the hemipteran Oncopeltus fasciatus (the large milkweed bug). Individuals depleted for 29 Dnmt1, and subsequently DNA methylation, failed to reproduce. Eggs were inviable and 30 declined in number, and nuclei structure of follicular epithelium was aberrant. Depletion 31 of DNA methylation did not result in changes in gene or transposable element expression 32 revealing an important function of DNA methylation seemingly not contingent on gene 33 expression. Our work provides direct experimental evidence for a functional role of 34 Dnmt1 and DNA methylation independent of gene expression in insects.

35

### 36 Introduction

37

38 DNA methylation in insects has been hypothesized to play numerous functional 39 roles including polyphenism, diapause, longevity, and social behavior and caste 40 differentiation [1–21]. However, these hypotheses are based primarily on correlational 41 studies; for example, there is evidence that the dependence of social behavior and caste 42 differentiation on DNA methylation is not absolute [11–13]. Comparative epigenomic 43 studies have provided valuable insights into patterns of DNA methylation across most 44 insects, but have offered limited insights into its functional significance.

45 In animals DNA methylation typically occurs at CG sites, which is established by 46 methyltransferase 3 (Dnmt3), and subsequently maintained by DNA DNA 47 methyltransferase 1 (Dnmt1). Many insects possess Dnmt1 and Dnmt3; however, there is 48 variation in presence-absence and copy number of these DNA methyltransferases, and 49 levels and patterns of DNA methylation [12, 13]. In many insects DNA methylation is 50 localized to moderately and constitutively expressed genes that are highly conserved 51 between species. This has led some to the hypothesis that DNA methylation functions in 52 transcriptional regulation [6, 15, 22, 23]. However, functional tests of DNA 53 methyltransferases in insects are limited to the post-transcriptional knock down of *Dnmt3* 54 in Apis mellifera, which is associated with modest reductions in DNA methylation, 55 differential gene expression, and alternative splicing [24]. Given the variation in 56 mechanisms that establish and maintain DNA methylation and limited genetic and mutant 57 studies, the function of insect DNA methyltransferases, and DNA methylation itself, is 58 obscure.

59 Here we show that DNA methylation is maintained by *Dnmt1*, is essential and is 60 not associated with transcription in the hemipteran Oncopeltus fasciatus (the large 61 milkweed bug) [25, 26]. Post-transcriptional knockdown of *Dnmt1* led to reduced egg 62 viability, fecundity, and aberrant follicular epithelium, and thus failure to produce a 63 successive generation. Despite finding levels of methylated CG (mCG) within coding 64 regions reduced by 83.55%, we found no evidence for DNA methylation directly 65 affecting transcription. Our results suggest *Dnmt1* plays an important role in reproduction 66 in O. fasciatus that is mediated by a gene-regulatory independent function of DNA 67 methylation. Oncopeltus fasciatus represents a fruitful model species for functional

studies of DNA methylation, and continuation of studies in this system will unravel theinsect epigenome and its functional consequences.

70

71 **Results** 

72

73 **Dnmt1** is necessary for reproduction. To assess the function of Dnmt1, double-stranded 74 RNA (dsRNA) targeting *Dnmt*1 (ds-*dnmt*1) (S1 Fig, and S1 and S2 Tables) was injected 75 between the abdominal sternites of virgin O. fasciatus females. Maternal dsRNA 76 injection has been used in O. fasciatus to post-transcriptionally knockdown expression in 77 embryos developing from eggs laid by injected females [27] and is known to reduce 78 expression of embryonically expressed genes. A control injection of double-stranded Red 79 (ds-red) or buffer was used to confirm that there was no technical affect associated with 80 RNAi treatment. The effects of RNAi treatment on gene expression was assessed in gut, 81 head, thorax and ovary tissues 10 days after mating to untreated O. fasciatus males. The 82 post-transcriptional knockdown reduced *dnmt1* mRNA expression in all examined tissues 83 (Fig 1A, and S2 Fig and S2 Table). Moreover, there was little variation in expression 84 between biological replicates in ds-dnmt1-injected and control individuals (Fig 1A). 85 Taken together, treatment with ds-dnmt1 specifically and reliably knocked down Dnmt1 86 transcripts.

87

Fig. 1. Dnmt1 is required for reproduction in O. fasciatus. (A) Assessment of RNAi
treatment targeting Dnmt1 using qRT-PCR demonstrates successful reduction in
transcription in ovaries compared to control. Dots indicate mean expression level, and

91 error bars indicate standard error of the mean. (B) Parental RNAi injection with ds-dnmt1 92 significantly affected the development of eggs laid by injected females compared to eggs 93 laid by control females. Dots indicate mean expression level, and error bars indicate 94 standard error of the mean. (C) Whole ovaries from females removed 12-14 days post-95 injection (i and ii). In control females (i), mature oocytes can be seen collecting in the 96 lateral oviduct (Od). In ds-dnmt1 females (ii), no mature oocytes are apparent, but the 97 oviduct has filled with a yolk-like substance. Scale bar equals 1 mm in (i) and (ii). High 98 magnification of the follicular epithelium surrounding a maturing oocyte (iii and iv). 99 Nuclei are stained with Hoechst 33258 and artificially colored turquoise. Nuclei from 100 control follicular epithelium (iii) are round and regular in shape. Nuclei from ds-dnmt1 101 females (iv) are highly irregular in shape.

102

103 Post-transcriptional knockdown of *Dnmt1* affects egg development and viability. 104 In the early stages following injection, females injected with ds-dnmt1 did not lay fewer 105 eggs (F = 2.91, df = 1; p = 1.1e-01) (S3 Fig). Although eggs laid by females injected with 106 ds-*dnmt1* within the first 8 days post-injection looked typical, they were significantly less likely to develop than the eggs laid by control females ( $\chi^2 = 8.470$ ; df = 1; p = 4.0e-03). 107 108 Furthermore, a mean of 93% of the eggs laid by control females initiated development 109 whereas only a mean of 4% of the eggs laid by ds-dnmt1 females initiated development 110 (Fig 1B). Although eggs laid by the control females that initiated development were 111 viable and hatched, the few eggs laid by ds-dnmt1-injected females that initiated 112 development were not viable and failed to hatch.

113 Post-transcriptional knockdown of *Dnmt1* affects egg production following the 114 first 10-day post-injection. By 10 to 12 days, females injected with ds-*dnmt1* have mainly 115 stopped laying eggs. While ovaries dissected from control females at this stage have 116 intact eggs in the oviduct, the oviducts of ds-*dnmt1*-injected females are either empty or 117 filled with a mass of what appears to be yolk (Fig 1C), indicating a fault in production of 118 a functional chorion. Analysis of ovarian cell structure indicates that knockdown of 119 Dnmt1 transcripts affects the cell structure of the follicular epithelium, which is 120 responsible for production of the chorion and vitelline envelope. Nuclei of the follicular 121 epithelium in *Dnmt1* post-transcriptional knock downed females are aberrant and fewer 122 in number than that of the control females (Fig 1C). Therefore, both through disruption of 123 embryonic development from eggs produced within a week of injection and cessation of 124 egg production, reproduction is compromised following knockdown of Dnmt1 125 transcripts, preventing a successive generation.

126

127 Post-transcriptional knock down of Dnmt1 successfully and severely reduces mCG 128 in ovaries. The successful knockdown of *Dnmt1* transcripts in gut, head, thorax and 129 ovaries prompted the evaluation of the consequences on DNA methylation using whole 130 genome bisulfite sequencing (WGBS). We used a low coverage sequencing approach, 131 which is sufficient for the detection of changes in bulk levels of DNA methylation [28]. 132 Although *Dnmt1* mRNA expression was reduced in all tissues, DNA methylation was 133 only reduced in ovary tissue (Fig 2A–C and S2 Fig). The reduction specifically in ovaries 134 is likely due to the higher rate of cell division in comparison to cells in other tissues surveyed, which would facilitate the passive of loss of DNA methylation in the absenceof *Dnmt1*.

137

Fig. 2. *Dnmt1* is required for mCG in *O. fasciatus*. (A) Level and genomic location of mCG between hemi– and holometabolous insects, and *D. pulex*, and RNAi treatment targeting *Dnmt1* in *O. fasciatus*. (B) Levels of mCG across gene bodies and one kilobase pairs (1kb) flanking sequence of hemi– and holometabolous insects, and *D. pulex*. Also shown are the levels of mCG across gene bodies for *O. fasciatus* ds-*dnmt1*. (C) Density plot representation of mCG for RNAi treated *O. fasciatus* and species investigated in this study.

145

146 High coverage single-base resolution DNA methylomes from ds-dnmt1 and 147 control ovaries were generated to understand the impact of the loss of Dnmt1. Greater 148 than 75% reductions of mCG were observed across the genome, consistent with the 149 decrease observed in the low coverage experiments (S2 Fig). The presence of 150 symmetrical mCG – DNA methylation occurring on both DNA strands at a CpG site – is 151 indicative of the presence of a functional *Dnmt1*. In control individuals methylation at 152 CpGs is highly symmetrical and highly methylated. However, even though knockdown of 153 Dnmt1 significantly reduces methylation in ovaries, a minority of CpG sites remain 154 symmetrically methylated (Fig 2C). This suggests that there are some cells within ovaries 155 that have wild-type methylomes. The lack of a complete loss of mCG is expected due to 156 the injection of fully developed individuals and hence the presence of fully methylated 157 genomes that existed prior to the injection of dsRNA.

158 Comparative epigenomic analysis of the O. fasciatus methylome with other insects. 159 The O. fasciatus methylome revealed much higher levels of mCG throughout the 160 genome, similar to other hemimetabolous insects, when compared to holometabolous 161 insects (Fig 2A and B). DNA methylation of gene bodies is found in O. fasciatus similar 162 to other insects that possess DNA methylation, however, the pattern of mCG within 163 exonic regions of hemi– and holometabolous insects is distinct (Fig 2B). Higher levels of 164 mCG are towards the 5' end compared to the 3' end of coding regions in holometabolous 165 insects. This distribution resembles the most recent common ancestor of all insects 166 (crustaceans) represented by *Daphnia pulex*. Hemimetabolous insects, which include O. 167 fasciatus, have a more uniform distribution of mCG across coding regions, and higher 168 levels towards the 3' end of coding regions. Previous studies have demonstrated that CG-169 methylated genes are often conserved within insects. We identified 39.31% (N = 7,561) 170 CG-methylated genes in O. fasciatus and 85.99% of these are CG-methylated in at least 171 one other insect species investigated (S3 Table). Therefore, even though the pattern of 172 DNA methylation within gene bodies of hemimetabolous insects is distinct compared to 173 holometabolous insects, the targeting of specific genes is conserved. Thus, the reductions 174 of mCG across gene bodies in ds-*dnmt1* individuals provides an apportunity to study its 175 potential function.

176

177 Decreased levels of mCG are not associated with transcriptome-wide changes in 178 gene or transposable element expression in ovaries. We performed RNA-seq analysis 179 from ovary and other tissues in ds-*dnmt1* and control individuals to better understand the 180 relationship between gene expression and DNA methylation. No relationship between

discrete mCG levels and gene expression was observed and this was consistent in other insects that we investigated (Fig 3A, and S4 Fig and S4–7 Tables). Furthermore, no correlation between continuous mCG levels and gene expression was observed (Fig 3B, and S4 Fig and S4–7 Tables). Interestingly, genome-wide relationships between DNA methylation and gene expression were not impacted by the knockdown of *Dnmt1* transcripts (Fig 3B).

187

188 Fig. 3. Loss of mCG in *O. fasciatus* ovaries has a limited effect on transcription. (A) 189 Gene expression level for deciles of increasing mCG (1-10) and unmethylated genes 190 (UM). Error bars represent 95% confidence interval of the mean. (B) Regression of gene 191 expression against a continuous measure of mCG with > 0 FPKM for the same set of 192 genes that are CG-methylated in O. fasciatus control, but unmethylated in ds-dnmt1. Raw 193 p values are provided for each regression, and significance or non-significance (NS) is 194 indicated in brackets following Bonferroni correction. (C) Combinational overlap of 195 genes that are differential CG-methylated and expressed, and similarly CG-methylated 196 and expressed between O. fasciatus ds-dnmt1 and control. Gene groups: Differentially 197 Methylated Gene (DMG), Differentially Expressed Gene (DEG), Similarly Methylated 198 Gene (SMG)/UnMethylated Genes (UMG), and non-Differentially Expressed Gene (non-199 DEG). (D) A heatmap showing gene expression changes for genes that are differentially 200 CG-methylated between O. fasciatus ds-dnmt1 and control. Expression was standardized 201 by the highest value per gene per biological replicate to produce a Relative Fragments Per 202 Kilobase of transcript per Million (RFPKM) value. RFPKM were clustered using a 203 hierarchical clustering method.

204 A maximum of 264 differentially expressed genes (DEG) were observed between 205 O. fasciatus ds-dnmt1 and control ovaries (S5 Table). Dnmt1 was down-regulated in all 206 ds-dnmt1 samples and no detection of the de novo DNA methyltransferase Dnmt3 was 207 observed. Additionally, no DEGs are observed between O. fasciatus ds-dnmt1 and 208 control for gut, head and thorax (S8 Table). Of genes with differences in DNA 209 methylation between ds-dnmt1 and control ovaries (N = 6,590), the majority (N = 6,484; 210 98.39%) had no changes to gene expression (Fig 3C, and S4 and S5 Tables). 211 Furthermore, mCG was always reduced in ds-*dnmt1* compared to control ovaries in the 212 6,484 gene set. Despite genes being unmethylated (UM) in ds-dnmt1 ovaries, changes to 213 gene expression occurred in both directions for the 106 differentially DNA methylated 214 and expressed genes (Fig 3D). Even for genes that by definition are unmethylated (N =215 5,982) or similarly CG-methylated (N = 21) in ds-dnmt1 and control, a similar proportion 216 (N = 6,003; 97.53%) was observed to have no difference in gene expression. The lack of 217 an association between DNA methylation and gene expression is further supported when 218 applying more stringent thresholds to the definition of CG-methylated and unmethylated 219 genes (S5 Fig). Our observations support a trivial role of DNA methylation in gene 220 expression if any at all.

The function of DNA methylation in *O. fasciatus* might lie within genome defense – the transcriptional regulation of repetitive DNA and transposons – as its genome is composed of a nontrivial amount of repetive DNA and transposons (6.21%) (S9 Table). However, as in genes, reduction of mCG in ds-*dnmt1* compared to control ovaries was found across the bodies of the TEs, and were not associated with a genome-

wide increase in expression (Fig 4A–C, and S6 Fig and S10 Table). This further supportsa trivial role of DNA methylation in transcriptional regulation of loci.

228

230

## Fig. 4. Large-scale reactivation of TEs did not follow severe reductions of mCG in

231 500 bp in the *O. fasciatus* genome. The dashed lines correspond to the intergenic mCG

**O.** fasciatus ovaries. (A) CG methylation levels for the top ten most abundant TEs of  $\geq$ 

level of *O. fasciatus* ds-*dnmt1* and control. (B) Levels of mCG across the bodies and 1kb

233 flanking sequence of TEs for a single representative of DNA transposons (Chapaev),

234 LTR retrotransposons (Gypsy), and non-LTR retrotransposons (Jockey). (C) Expression

235 quantified as RPKM for the top ten most abundant TEs of  $\geq$  500 bp. The subset presents

the RPKM distribution when all TEs are considered within ds-*dnmt1* and control ovaries.

237

## 238 Discussion

239

DNA methylation has been implicated to play numerous roles in insects [1–21], however, its exact function remains uncertain. In this study we observed that posttranscriptional knockdown of *Dnmt1* negatively impacts reproduction through a decrease in egg development and egg production in *O. fasciatus*.

Post-transcriptional knockdown of *Dnmt1* transcripts impacted the maternal somatic gonad and egg maturation. The follicular epithelial cells undergo multiple rounds of mitosis during oogenesis [29]. Oocytes that were in the early stages of maturation would be the most effected, as their follicular epithelium would passively lose DNA methylation with each successive round of mitotis. Loss was not compensated by the *de*  *novo* DNA methyltransferase *Dnmt3* as expression was not observed in ovaries. The loss
of function of follicular epithelial cells, which includes production of the chorion and
vitelline membrane, could explain the loss of oocyte integrity.

The knockdown of *Dnmt1* transcripts in *O. fasciatus* ovaries subsequently did not lead to transcriptome-wide changes in gene expression. No correlation between mCG and gene expression in *O. fasciatus* ovaries and other insects was observed (Fig 3 and S4 Fig) [6, 13]. Hence, the importance of mCG in *O. fasciatus* might lie within the orchestration of genomic structure during cell replication, gametogenesis, or cell types not examined in our study.

258 DNA methylation might be required for proper mitosis, and the segration of sister 259 chromatids into their respective daughter cells, as there does appear to be aberrant nuclei 260 structure in ds-dnmt1 compared to control ovarian cells (Fig. 1C). This phenotype could 261 be the result of epigenomic defects in scaffold/matrix attachment regions (S/MAR), as 262 some correlate with origins of replication [30]. This phenotype could be exacerbated by 263 multiple mitotic divisions of follicular epithelial cells during oogenesis, and/or the 264 presence of holocentric chromosomes [31]. Future work describing the epigenomic 265 contributions to cellular defects are now possible to study in this newly emerging and 266 tractable model species, O. fasciatus.

We suggest that DNA methylation is more important for genome structure, integrity or other cellular processes than it is for somatic expression in *O. fasciatus*. Although it is possible that DNA methylation is important for expression control in a rare cell type that was not examined in our study, we instead propose that regulation of expression is not likely the primary role in insects. Investigating the importance of DNA

272	methylation prior to the onset of meiosis and throughout embryo development is a
273	fundamental next-step. Oncopeltus fasciatus represents a fruitful model species for
274	functional studies of DNA methylation, and continuation of studies in this system will
275	unravel the insect epigenome and its functional consequences.
276	
277	Materials and Methods
278	
279	Phylogenetic analysis. A subset of DNA methyltransferase (Dnmt) 1, 2, and 3 sequences
280	was obtained from [16] for phylogenetic analysis. The subset included only insect species
281	with available MethylC-seq data, and species representatives from the dipteran suborders
282	Brachycera and Nematocera: Acyrthosiphon pisum, Aedes aegypti, Aedes albopictus,
283	Anopheles gambiae, Apis mellifera, Bombyx mori, Camponotus floridanus, Copidosoma
284	floridanum, Culex pipiens quinquefasciatus, Drosophila melanogaster, Harpegnathos
285	saltator, Microplitis demolitor, Nasonia vitripennis, Nicrophorus vespilloides, O.
286	fasciatus, Ooceraea (Cerapachys) biroi, Polistes canadensis, Polistes dominula,
287	Solenopsis invicta, Tribolium castaneum, and Zootermopsis nevadensis. DNA
288	methyltransferases were reassessed in O. fasciatus by using InterProScan v5.23-62.0 [32]
289	to identify annotated proteins with a C-5 cytosine-specific DNA methylase domain
290	(PF00145). Sequence identifiers are located in S1 Fig. Full-length protein sequences were
291	aligned using PASTA v1.6.4 [33], and manually trimmed of divergent, non-homologous
292	sequence in Mesquite v3.2 [34]. Full, aligned, and aligned and trimmed sequence
293	alignments, and parenthetical phylogenetic tree are located in S1 Data. Phylogenetic
294	relationship among Dnmt sequences was estimated using BEAST v2.3.2 [35] with a

Blosum62+Γ model of amino acid substitution. A Markov Chain Monte Carlo (MCMC)
was ran until stationarity and convergence was reached (10,000,000 iterations), and a
burnin of 1,000,000 was used prior to summarizing the posterior distribution of tree
topologies. A consensus tree was generated using TreeAnnotator v2.3.2, visualized in
FigTree v1.4.2 (http://tree.bio.ed.ac.uk/software/figtree/) and exported for stylization in
Affinity Designer v1.5.1 (https://affinity.serif.com/en-us/).

301

PCR confirmation for the presence of a single *Dnmt1* ortholog in *O. fasciatus*. To determine if OFAS015351 and OFAS018396 were two parts of a single *Dnmt1* ortholog, we designed one sense primer at the 3' end of OFAS015351 (Of\_DMNT1-1\_3603S; S1 Table) and two antisense primers at the 3' end of OFAS018396 (Of\_DNMT1-2\_424A and Of\_DNMT1-2\_465A; S1 Table). A fourth sense primer (Of\_DNMT1-2\_1S; S1 Table) was designed at the 5' end of OFAS018396 to confirm the size and sequence of this possibly truncated gene annotation.

309 Polymerase Chain Reaction (PCR) with primer combinations Of\_DMNT1-310 1\_3603S-Of\_DNMT1-2\_424A, Of\_DMNT1-1\_3603S-Of\_DNMT1-2\_465A, and 311 Of\_DNMT1-2\_1S-Of\_DNMT1-2\_424A was performed using Q5 Polymerase (New 312 England BioLabs, Ipswich, MA) per manufactures instructions. Thermacycler conditions 313 were 98°C for 15 seconds (s) (denaturing), 60°C for 30 s (annealing), and 72°C for 30 s 314 (extension), and repeated for 40 cycles. The PCR products were then purified using 315 QIAquick PCR Purification Kit (Qiagen, Venlo, The Netherlands), and sequenced at the 316 Georgia Genomics and Bioinformatics Core (Athens, GA).

Animal culture. *Oncopeltus fasciatus* cultures were originally purchased from Carolina Biologicals (Burlington, NC). Mass colonies were maintained in incubators under a 12 h:12 h light/dark cycle at 27°C. Colonies and individual experimental animals were fed organic raw sunflower seeds and provided with *ad libitum* deionized water. Late instar nymphs were separated from the mass colonies and housed under the same conditions. Nymph colonies were checked daily for newly emerged adults. Adults were separated by sex and kept with food and water for 7–10 days until females reached sexual maturity.

325

326 **Parental RNAi.** Template for the *in vitro* transcription of reactions was prepared from a 327 PCR reaction in which T7 phage promoter sequences were added to the gene-specific 328 Dnmt1 primers [36]. For our control sequence, we used the red fluorescent protein (Red) 329 sequence used in previous parental RNAi experiments in O. fasciatus [36] or buffer. 330 Primer sequences can be found in S2 Table. Sense and anti-sense RNA was synthesized 331 in a single reaction using the Ambion MEGAscript kit (ThermoFisher Sci, Waltham, 332 MA). After purification, the double-stranded RNA (dsRNA) concentration was adjusted 333 to 2  $\mu$ g/ $\mu$ L in injection buffer (5 mM KCl, 0.1 mM NaH<sub>2</sub>PO<sub>4</sub>) [36]. Females were 334 injected with 5  $\mu$ L of dsRNA between the abdominal sternites using an insulin syringe. 335 Following injection, females were paired with an un-injected male to stimulate 336 oviposition and fertilize eggs. Individual females with their mate were housed in petri 337 dishes with sunflower seeds, water and cotton wool as an oviposition site. The parental 338 RNAi protocol has been reported to result in 100% penetrance by the third clutch of eggs 339 [36] and this was also our experience.

340

341 **Reproductive phenotype screening and analysis.** Eggs were collected between days 4– 342 10 post-injection and assessed for development. Oncopeltus fasciatus embryos change 343 from a creamy white color to orange as they develop, which indicates viability. Thus, 344 color change is a useful tool for assessing healthy development. We examined the 345 number of developing eggs at 5 days post-oviposition, at which point viable eggs are 346 clearly distinguishable from inviable eggs, as well as hatching rate of eggs from females 347 injected with double-stranded Dnmt1 (ds-dnmt1) and double-stranded Red (ds-red). The 348 data for the number of eggs laid was normally distributed so differences among RNAi 349 treated groups were tested using analysis of variance (ANOVA). The development data, 350 however, was not normally distributed and consisted of binary states (developed and not 351 developed), and so differences among treatment groups were analyzed with a Generalized 352 Linear Model (GLM) using a Poisson distribution.

353 A second set of O. fasciatus females were injected in the same manner as 354 described in **Parental RNAi** to assess post-transcriptional knockdown of *Dnmt1* on 355 ovarian structure. Oncopeltus fasciatus females were dissected 10 days after injection. By 356 10 days post-injection O. fasciatus females are beginning to stop laying recognizable 357 eggs. Ovaries were removed from O. fasciatus females and placed in  $1 \times PBS$ . Whole 358 ovaries were imaged with a Leica DFC295 stereomicroscope using Leica Application 359 Suite morphometric software (LAS V4.1; Leica, Wetzlar, Germany). Dissected ovaries 360 were fixed within 15 minutes of dissection in 4% formaldehyde in  $1 \times PBS$  for 25 361 minutes. Fixed ovaries were stained with Hoechst 33342 (Sigma Aldrich) at 0.5  $\mu$ g/ml. 362 The stained ovarioles were imaged using a Zeiss LSM 710 Confocal Microscope (Zeiss) 363 at the University of Georgia Biomedical Microscopy Core.

Quantitative RT-PCR. To assess the effectiveness of post-transcriptional knockdown of *Dnmt1*, females were dissected 11 days post-injection. Ovaries were removed from each
female, flash frozen in liquid nitrogen and stored at -80°C until processing. Total RNA
(and DNA) was extracted from a single ovary per female using a Qiagen Allprep
DNA/RNA Mini Kit (Qiagen, Venlo, The Netherlands) per manufacturer's instructions.
Complementary DNA (cDNA) was synthesized from 500 ng RNA with qScript cDNA
SuperMix (Quanta Biosciences, Gaithersburg, MD).

371 Expression level of *Dnmt1* was quantified by quantitative real-time PCR (qRT-372 PCR). Primers were designed for *Dnmt1* using the *O. fasciatus* genome as a reference 373 [37]. Actin and GAPDH were used as endogenous reference genes. Primer sequences can 374 be found in Extended Data Table 2. We used Roche LightCycler 480 SYBR Green 375 Master Mix with a Roche LightCycler 480 (Roche Applied Science, Indianapolis, IN) for 376 qRT-PCR. All samples were run with 3 technical replicates using 10 µL reactions using 377 the manufacturer's recommended protocol. Primer efficiency calculations, genomic 378 contamination testing and endogenous control gene selection were performed as 379 described by [37]. We used the  $\Delta\Delta$ CT method [38] to examine differences in expression 380 between control and ds-dnmt1 injected females [37].

381

Whole-Genome Bisulfite Sequencing (WGBS) and analysis of cytosine (DNA) methylation. MethylC-seq libraries for an *O. fasciatus* ds-*dnmt1* and control individual were prepared according to the protocol described in [39] using genomic DNA extracted from ovaries (see Materials and Methods section Quantitative RT-PCR). Libraries were single-end 75 bp sequenced on an Illumina NextSeq500 machine [40, 41].

387 Unmethylated lambda phage DNA was used to as a control for sodium bisulfite 388 conversion, and an error rate of ~0.05% was estimated. Oncopeltus fasciatus ds-dnmt1 389 and control were sequenced to a depth of  $\sim 18 \times$  and  $\sim 21 \times$ , which corresponded to an 390 actual mapped coverage of  $\sim 9 \times$  and  $\sim 11 \times$ , respectively. Additionally, low pass (< 1×) 391 WGBS from gut, head, ovary, and thorax was performed for three control and ds-dnmt1 392 biological replicates. *Blattella germanica* was additionally sequenced to generate equal 393 numbers of hemi- and holometabolous insects investigated in this study. However, DNA 394 was extracted from whole-body minus gastrointestinal tract. MethylC-seq libraries were 395 prepared and sequenced identically to O. fasciatus. An error rate of  $\sim 0.14\%$  was 396 estimated from unmethylated lambda phage DNA. *Blattella germanica* was sequenced to 397 a depth of  $\sim 8\times$ , which corresponded to an actual mapped coverage of  $\sim 5\times$ . WGBS data 398 for O. fasciatus and B. germanica can be found on Gene Expression Omnibus (GEO) 399 under accession GSE109199. Previously published WGBS data for A. mellifera [42], Bo. 400 mori [17], Daphnia pulex [43], N. vespilloides [19], and Z. nevadensis [15] were 401 downloaded from the Short Read Archive (SRA) using accessions SRR445803-4, 402 SRR027157–9, SRR1552830, SRR2017555, and SRR3139749, respectively. Thus, DNA 403 methylation was investigated for six insects from six different orders spread evenly 404 across developmental groups, and a crustacean outgroup. WGBS data was aligned to each 405 species respective genome assembly using the methylpy pipeline [44]. In brief, reads 406 were trimmed of sequencing adapters using Cutadapt v1.9 [45], and then mapped to both 407 a converted forward strand (cytosines to thymines) and converted reverse strand 408 (guanines to adenines) using bowtie v1.1.1 [46]. Reads that mapped to multiple locations, 409 and clonal reads were removed.

410 Weighted DNA methylation was calculated for CG sites by dividing the total 411 number of aligned methylated reads by the total number of methylated plus unmethylated 412 reads [47]. For genic metaplots, the gene body (start to stop codon), 1000 base pairs (bp) 413 upstream, and 1000 bp downstream was divided into 20 windows proportional windows 414 based on sequence length (bp). Weighted DNA methylation was calculated for each 415 window and then plotted in R v3.2.4 (https://www.r-project.org/). CG sequence context 416 enrichment for each gene was determined through a binomial test followed by Benjamini-417 Hochberg false discovery rate [48, 49]. A background mCG level was determined from 418 all coding sequence, which was used as a threshold in determining significance with a 419 False Discovery Rate (FDR) correction. Genes were classified as CG-methylated if they 420 had reads mapping to at least 20 reads mapping to 20 CG sites and a q < 0.05. Using a 421 binomial test can lead to false-negatives - highly CG-methylated genes that are classified 422 as unmethylated (UM) – due to a low number of statistically CG-methylated sites (S4 423 Table). Genes classified as unmethylated, but had a mCG level greater than the lowest 424 CG-methylated gene were dropped from future analyses.

425

426 Ortholog identification. Best BLASTp hit (arguments: -max\_hsps 1 –max\_target\_seqs 1
427 evalue 1e-03) was used to identify orthologs between *O. fasciatus* and other insect
428 species investigated.

429

RNA-seq and differential expression analysis. RNA-seq libraries for RNA extracted
from ovaries of three biological *O. fasciatus* ds-*dnmt1* and control replicates at 11 days
post-injection were constructed using Illumina TruSeq Stranded RNA LT Kit (Illumina,

433 San Diego, CA) following the manufacturer's instructions with limited modifications. 434 RNA from ovaries of an additional three biological O. fasciatus ds-dnmt1 and control 435 replicates, and three biological O. fasciatus ds-dnmt1 and control replicates from gut, 436 head, and thorax were extracted. The starting quantity of total RNA was adjusted to 1.3 437  $\mu$ g, and all volumes were reduced to a third of the described quantity. Libraries were 438 single-end 75 bp sequenced on an Illumina NextSeq500 machine. RNA-seq data for O. 439 fasciatus ds-dnmt1 and control can be found on GEO under accession GSE109199. 440 Previously published RNA-seq data for A. mellifera [50], and Z. nevadensis (15) were 441 downloaded from the SRA using accessions SRR2954345, and SRR3139740, 442 respectively.

Raw RNA-seq FASTQ reads were trimmed for adapters and preprocessed to remove low-quality reads using Trimmomatic v0.33 (arguments: LEADING:10 TRAILING:10 MINLEN:30) [51] prior to mapping to the *O. fasciatus* v1.1 reference genome assembly. Reads were mapped using TopHat v2.1.1 [52] supplied with a reference General Features File (GFF) to the *O. fasciatus* v1.1 reference genome assembly [26], and with the following arguments: -I 20000 --library-type fr-firststrand -b2-very-sensitive.

Differentially expressed genes (DEGs) between ds-*dnmt1* and control libraries were determined using edgeR v3.20.1 [53] implemented in R v3.2.4 (<u>https://www.r-</u> project.org/). Genes were retained for DEG analysis if they possessed a Counts Per Million (CPM)  $\geq$  1 in at least  $\geq$  2 libraries. Significance was determined using the glmQLFTest function, which uses empirical Bayes quasi-likelihood F-tests. Parameter settings were determined following best practices for DEG analysis as described by [54].

456 Gene expression metrics for *A. mellifera*, *Z. nevadensis*, and *O. fasciatus* ds-*dnmt1* and 457 control are located in S5–8 Tables, respectively.

458

459 Gene Ontology (GO) annotation and enrichment. GO terms were assigned to O. 460 fasciatus v1.1 gene set [26] through combining annotations from Blast2Go PRO v4.1.9 461 [55], InterProScan v5.23-62.0 (arguments: -goterms -iprlookup -appl CDD,Pfam) [32], 462 and through sequence homology to *D. melanogaster* using BLASTp (arguments: -evalue 463 1.0e-03 -max target seqs 1 -max hsps 1). 11,105/19,615 gene models were associated 464 with at least one GO term and a total of 8,190 distinct GO identifiers were mapped. GO 465 terms are found in S11 Table. Enriched GO terms in gene groups were evaluated using 466 topGO v2.30.0 [56] implemented in R v3.2.4 (https://www.r-project.org/), and 467 significance (p < 0.05) of terms was assessed using Fisher's exact test with a weighted 468 algorithm. Gene groups were contrasted to all O. fasciatus genes associated with GO 469 terms (S12 Table).

470

471 Transposable element (TE) annotation and expression. TEs were identified using 472 RepeatMasker v4.0.5 (<u>http://www.repeatmasker.org</u>) provided with the invertebrate 473 repeat library from Repbase (<u>http://www.girinst.org/repbase/</u>) (arguments: -lib <Repbase 474 invertebrate library> -no\_is -engine wublast -a -inv -x -gff. Following RepeatMasker, 475 neighboring TEs of the same type were collapsed into a single locus within the outputted 476 GFF. The unmodified GFF is located in S9 Table.

To quantify expression from TEs RNA-seq libraries from *O. fasciatus* ds-*dnmt1* and control were independently combined and mapped to the *O. fasciatus* v1.1 reference

479 genome assembly [26] using bowtie2 v2.2.9 [57] with the following arguments: --480 sensitive. Mapped reads overlapping with the top ten most abundant TEs of  $\geq$  500 bp in 481 length were identified using the *intersect* command in BEDTools suite v 2.26.0 [58]. TE 482 expression is quantified as Reads Per Kilobase per Million mapped reads (RPKM) for 483 each intersected TE type by counting the number reads and dividing by the mapped 484 library read number in millions. Significance in expression of TEs between ds-dnmt1 and 485 control tissues was assessed using the Mann-Whitney test with the alternative hypothesis 486 set to "greater" in R v3.2.4 (https://www.r-project.org/).

487

## 488 Acknowledgements

489

490 We thank Sam Arsenault (University of Georgia [UGA]), and Mariana Monteiro 491 and Stefan Götz (Blast2GO Team) for assistance with Blast2GO analyses, Nick Rohr and 492 Tina Ethridge for MethylC-Seq and RNA-seq library preparation, Brigitte Hofmeister 493 (UGA) for bioinformatics advice, Mary Goll (UGA) for comments, Kelly Dawe (UGA) 494 for feedback on cellular phenotypes, Muthugapatti Kandasamy of the Biomedical 495 Microscopy Core (UGA) for technical assistance with confocal microscopy, and 496 Cassandra Extavour (Harvard) for providing technical advice and Red plasmids for 497 RNAi. We also thank the Georgia Advanced Computing Resource Center (GACRC), 498 Georgia Genomics and Bioinformatics Core (GGBC) and the Office of Research at the 499 University of Georgia. This work was funded by the National Science Foundation (NSF) 500 IOS-1354358 (AJM), and UGA CAES Undergraduate Research Award (ZS). RJS is a 501 Pew Scholar in the Biomedical Sciences, supported by The Pew Charitable Trusts.

## 502 **References**

- Falckenhayn C, Boerjan B, Raddatz G, Frohme M, Schoofs L, Lyko F.
   Characterization of genome methylation patterns in the desert locust *Schistocerca*
- 506 *gregaria*. J Exp Biol. 2013;216: 1423–1429.
- 2. Cullen DA, Cease AJ, Latchininsky AV, Ayali A, Berry K, Buhl J, et al. From
  molecules to management: mechanisms and consequences of locust phase
  polyphenism. Adv In Insect Phys. 2017;53: 167–285.
- 510 3. Pegoraro M, Bafna A, Davies NJ, Shuker DM, Tauber E. DNA methylation changes
- 511 induced by long and short photoperiods in *Nasonia*. Genome Res. 2016;26: 203–210.
- 512 4. Reynolds JA. Epigenetic influences on diapause. Adv In Insect Phys. 2017;53: 115–
  513 144.
- 5. Kozeretska IA, Serga SV, Koliada AK, Vaiserman AM. Epigenetic regulation of
  longevity in insects. Adv In Insect Phys. 2017;53: 87–114.
- 516 6. Bonasio R, Li Q, Lian J, Mutti NS, Jin L, Zhao H, et al. Genome-wide and caste-
- 517 specific DNA methylomes of the ants *Camponotus floridanus* and *Harpegnathos*518 *saltator*. Curr Biol. 2012;22: 1755–1764.
- 519 7. Foret S, Kucharski R, Pellegrini M, Feng S, Jacobsen SE, Robinson GE, et al. DNA
  520 methylation dynamics, metabolic fluxes, gene splicing, and alternative phenotypes in
- 521 honey bees. Proc Natl Acad Sci USA. 2012;109: 4968–4973.
- 522 8. Lockett GA, Kucharski R, Maleszka R. DNA methylation changes elicited by social
- 523 stimuli in the brains of worker honey bees. Genes Brain Behav. 2012;11: 235–242.

- 524 9. Ford D. Honeybees and cell lines as models of DNA methylation and aging in
  525 response to diet. Exp Gerontol. 2013;48: 614–619.
- 526 10. He XJ, Zhou LB, Pan QZ, Barron AB, Yan WY, Zeng ZJ. Making a queen: an
- 527 epigenetic analysis of the robustness of the honeybee (Apis mellifera) queen
- developmental pathway. Mol Ecol. 2017;26: 1598–1607.
- 529 11. Libbrecht R, Oxley PR, Keller L, Kronauer DJ. Robust DNA methylation in the
  530 clonal raider ant brain. Curr Biol. 2016;26: 391–395.
- 531 12. Bewick AJ, Vogel KJ, Moore AJ, Schmitz RJ. Evolution of DNA methylation across
  532 insects. Mol Biol Evol. 2016;34: 654–665.
- 533 13. Glastad KM, Arsenault SV, Vertacnik KL, Geib SM, Kay S, Danforth BN, et al.
- Variation in DNA methylation is not consistently reflected by sociality in
  Hymenoptera. Genome Biol Evol. 2017;9: 1687–1698.
- 536 14. Provataris P, Meusemann K, Niehuis O, Grath S, Misof M. Signatures of DNA
- 537 methylation across insects suggest reduced DNA methylation levels in Holometabola.
- 538 Genome Biol Evol. 2018;10: 1185–1197.
- 539 15. Glastad KM, Gokhale K, Liebig J, Goodisman MAD. The caste- and sex-specific
- 540 DNA methylome of the termite *Zootermopsis nevadensis*. Sci Rep. 2016;6: 37110.
- 541 16. Lyko F, Foret S, Kucharski R, Wolf S, Falckenhayn C, Maleszka R. The honey bee
- 542 epigenomes: differential methylation of brain DNA in queens and workers. PLoS543 Biol. 2010;8 :e1000506.
- 544 17. Xiang H, Zhu J, Chen Q, Dai F, Li X, Li M, et al. Single base-resolution methylome
- of the silkworm reveals a sparse epigenomic map. Nat Biotechnol. 2010;28: 516–520.

- 546 18. Wang X, Wheeler D, Avery A, Rago A, Choi JH, Colbourne JK, et al. Function and
  547 evolution of DNA methylation in *Nasonia vitripennis*. PLoS Genet. 2013;9:
  548 e1003872.
- 549 19. Cunningham CB, Ji L, Wiberg RA, Shelton J, McKinney EC, Parker DJ, et al. The
- 550 genome and methylome of a beetle with complex social behavior, *Nicrophorus*
- 551 *vespilloides* (Coleoptera: Silphidae). Genome Biol Evol. 2015;7: 3383–3396.
- 552 20. Patalano S, Vlasova A, Wyatt C, Ewels P, Camara F, Ferreira PG, et al. Molecular
- signatures of plastic phenotypes in two eusocial insect species with simple societies.
- 554 Proc Natl Acad Sci USA. 2015;112: 13970–13975.
- 555 21. Rehan SM, Glastad KM, Lawson SP, Hunt BG. The genome and methylome of a
- subsocial small carpenter bee, *Ceratina calcarata*. Genome Biol Evol. 2016;8: 1401–
  1410.
- 558 22. Sarda S, Zeng J, Hunt BG, Yi SV. The evolution of invertebrate gene body
  559 methylation. Mol Biol Evol. 2012;29: 1907–1916.
- 560 23. Hunt BG, Glastad KM, Yi SV, Goodisman MAD. Patterning and regulatory
- associations of DNA methylation are mirrored by histone modifications in insects.
- 562 Genome Biol Evol. 2013;5: 591–598.
- 563 24. Li-Byarlay H, Li Y, Stroud H, Feng S, Newman TC, Kaneda M, et al. RNA
  564 interference knockdown of DNA methyl-transferase 3 affects gene alternative
  565 splicing in the honey bee. Proc Natl Acad Sci USA. 2013;110: 12750–12755.
- 566 25. Chipman AD. *Oncopeltus fasciatus* as an evo-devo research organism. Genesis.
  567 2017;55.

- 568 26. Panfilio KA, Vargas Jentzsch IM, Benoit JB, Erezyilmaz D, Suzuki Y, Colella S, et
- al. Molecular evolutionary trends and feeding ecology diversification in the
- 570 Hemiptera, anchored by the milkweed bug genome; 2017. Preprint. Available from:
- 571 doi:<u>https://doi.org/10.1101/201731</u>. Cited 26 June 2018.
- 572 27. Liu PZ, Kaufman TC. Hunchback is required for suppression of abdominal identity,
- and for proper germband growth and segmentation in the intermediate germband
  insect *Oncopeltus fasciatus*. Development. 2004;131: 1515–1527.
- 575 28. Bewick AJ, Hofmeister BT, Lee K, Zhang X, Hall DW, Schmitz RJ. FASTmC: A
- 576 suite of predictive models for nonreference-based estimations of DNA methylation.
- 577 G3 (Bethesda). 2015;6: 447–752.
- 578 29. Bonhag PF, Wick JR. The functional anatomy of the male and female reproductive
- 579 systems of the milkweed bug, *Oncopeltus fasciatus* (Dallas) (Heteroptera:
  580 Lygaeidae). J Morphol. 1953;93: 177–283.
- 581 30. Vaughn JP, Dijkwel PA, Mullenders LH, Hamlin JL. Replication forks are associated
- 582 with the nuclear matrix. Nucleic Acids Res. 1990;18: 1965–1969.
- 583 31. Drinnenberg IA, deYoung D, Henikoff S, Malik HS. Recurrent loss of CenH3 is
- associated with independent transitions to holocentricity in insects. eLife. 2014;doi:
  10.7554/eLife.03676.
- 32. Jones P, Binns D, Chang HY, Fraser M, Li W, McAnulla C, et al. InterProScan 5:
  genome-scale protein function classification. Bioinformatics. 2014;30: 1236–1240.
- 588 33. Mirarab S, Nguyen N, Guo S, Wang LS, Kim J, Warnow T. PASTA: ultra-large
- 589 multiple sequence alignment for nucleotide and amino-acid sequences. J Comput
- 590 Biol. 2015;22: 377–386.

- 591 34. Maddison WP, Maddison DR. Mesquite: a modular system for evolutionary analysis.
- 592 Version 3.31. 2017;<u>http://mesquiteproject.org</u>.
- 593 35. Bouckaert R, Heled J, Kühnert D, Vaughan T, Wu CH, Xie D. et al. BEAST 2: a
- 594 software platform for Bayesian evolutionary analysis. PLoS Comput. Biol. 2014;10:
- e1003537.
- 596 36. Ewen-Campen B, Jones TE, Extavour CG. Evidence against a germplasm in the
  597 milkweed bug *Oncopeltus fasciatus*, a hemimetabolous insect. Biol Open. 2013;2:
  598 556–568.
- 599 37. Cunningham CB, Douthit MK, Moore AJ. Octopaminergic gene expression and
- flexible social behaviour in the subsocial burying beetle *Nicrophorus vespilloides*.
  Insect Mol Biol. 2014;23: 391–404.
- 602 38. Livak KJ, Schmittgen TD. Analysis of relative gene expression data using real-time
- 603 quantitative PCR and the 2(-Delta Delta C(T)) Method. Methods. 2001;25: 402–408.
- 39. Urich MA, Nery JR, Lister R, Schmitz RJ, Ecker JR. MethylC-seq library preparation
- for base-resolution whole-genome bisulfite sequencing. Nat Protoc. 2015;10: 475–
  483.
- 40. Cokus SJ, Feng S, Zhang X, Chen Z, Merriman B, Haudenschild CD, et al. Shotgun
  bisulphite sequencing of the *Arabidopsis* genome reveals DNA methylation
  patterning. Nature. 2008;452: 215–219.
- 610 41. Lister R, O'Malley RC, Tonti-Filippini J, Gregory BD, Berry CC, Millar AH, et al.
- 611 Highly integrated single-base resolution maps of the epigenome in *Arabidopsis*. Cell.
- 612 2008;133: 523–536.

- 613 42. Herb BR, Wolschin F, Hansen KD, Aryee MJ, Langmead B, Irizarry R, et al.
- 614 Reversible switching between epigenetic states in honeybee behavioral subcastes. Nat
- 615 Neurosci. 2012;15: 1371–1373.
- 43. Asselman J, De Coninck DIM, Pfrender ME, De Schamphelaere KAC. Gene body
- 617 methylation patterns in *Daphnia* are associated with gene family size. Genome Biol
- 618 Evol. 2016;8: 1185–1196.
- 619 44. Schultz MD, He Y, Whitaker JW, Hariharan M, Mukamel EA, Leung D, et al.
- 620 Human body epigenome maps reveal noncanonical DNA methylation variation.
- 621 Nature. 2015;523: 212–216.
- 45. Martin M, Marcel M. Cutadapt removes adapter sequences from high-throughput
  sequencing reads. EMBnet J. 2011;17: 10–12.
- 46. Langmead B, Trapnell C, Salzberg SL. Ultrafast and memory-efficient alignment of
  short DNA sequences to the human genome. Genome Biol. 2009;10: R25.
- 626 47. Schultz MD, Schmitz RJ, Ecker JR. 'Leveling' the playing field for analyses of single-
- base resolution DNA methylomes. Trends Genet. 2012;28: 583–585.
- 48. Takuno S, Gaut BS. Body-methylated genes in Arabidopsis thaliana are functionally
- 629 important and evolve slowly. Mol Biol Evol. 2012;1: 219–227.
- 49. Niederhuth CE, Bewick AJ, Ji L, Alabady MS, Kim KD, Li Q, et al. Widespread
  natural variation of DNA methylation within angiosperms. Genome Biol. 2016;17:
- 632194.
- 50. Vleurinck C, Raub S, Sturgill D, Oliver B, Beye M. Linking genes and brain
  development of honeybee workers: a whole-transcriptome approach. PLoS One.
  2016;11: e0157980.

- 51. Bolger AM, Lohse M, Usadel B. Trimmomatic: a flexible trimmer for Illumina
  sequence data. Bioinformatics. 2014;30: 2114–2120.
- 638 52. Kim D, Pertea G, Trapnell C, Pimentel H, Kelley R, Salzberg SL. TopHat2: accurate
- alignment of transcriptomes in the presence of insertions, deletions and gene fusions.
- 640 Genome Biol. 2013;14: R36.
- 641 53. Robinson MD, McCarthy DJ, Smyth GK. edgeR: a Bioconductor package for
- 642 ifferential expression analysis of digital gene expression data. Bioinformatics.
  643 2010;26: 139–140.
- 644 54. Chen Y, Lun ATL, Smyth GK. From reads to genes to pathways: differential
- expression analysis of RNA-Seq experiments using Rsubread and the edgeR quasilikelihood pipeline. F1000Res. 2016;5: 1438.
- 647 55. Götz S, García-Gómez JM, Terol J, Williams TD, Nagaraj SH, Nueda MJ, et al.
- High-throughput functional annotation and data mining with the Blast2GO suite.
  Nucleic Acids Res. 2008;36: 3420–3435.
- 56. Alexa A, Rahnenfuhrer J. topGO: Enrichment analysis for gene ontology. R package
  version 2.30.0. 2016.
- 57. Langmead B, Salzberg S. Fast gapped-read alignment with Bowtie 2. Nat Methods.
  2012;9: 357–359.
- 58. Quinlan AR, Hall IM. BEDTools: a flexible suite of utilities for comparing genomic
- 655 features. Bioinformatics. 2010;26: 841–842.

## 656 Supporting Information

657

658 S1 Fig. Identification of *O. fasciatus* DNA methyltransferases. (A) Phylogenetic 659 relationship of DNA methyltransferases identified the *de novo* (Dnmt3) and maintenance 660 (Dnmt1) DNA methyltransferase in O. fasciatus. Node support with  $\leq 0.5$  posterior 661 probability is indicated – other nodes are  $\geq 0.95$ . Branch lengths are in amino acid 662 substitutions per site. Species names are represented as abbreviations: Acy. pis.: 663 Acyrthosiphon pisum, Aed. aeg.: Aedes aegypti, Aed. alb.: Aedes albopictus, Ano. gam.: 664 Anopheles gambiae, Api. mel.: A. mellifera, Bom. mor.: Bo. mori, Cam. flo.: 665 Camponotus floridanus, Cop. flo.: Copidosoma floridanum, Cul. qui.: Culex pipiens 666 quinquefasciatus, Dro. mel.: Drosophila melanogaster, Har. sal.: Harpegnathos saltator, 667 Mic. dem.: Microplitis demolitor, Nas. vit.: Nasonia vitripennis, Nic. ves.: Nicrophorus 668 vespilloides, Onc. fas.: O. fasciatus, Cer. bir.: Ooceraea (Cerapachys) biroi, Pol. can.: 669 Polistes canadensis, Pol. dom.: Polistes dominula, Sol. inv.: Solenopsis invicta, Tri. cas.: 670 Tribolium castaneum, and Zoo. nev.: Z. nevadensis. (B) A to scale representation of 671 Dnmt1 and protein domains identified in O. fasciatus and M. musculus.

672

## 673 S2 Fig. DNA methylation consequences following post-transcriptional knockdown of

*Dnmt1* are restricted to ovaries. (A) Assessment of RNAi treatment targeting *Dnmt1*using qRT-PCR demonstrates successful reduction in transcription compared to control
across all tissues sampled. Colored dots indicate independent biological replicates. (B)
Genome-wide CG methylation level across tissues sampled. Numbers at the top of each
bar corresponds to independent biological replicates.

679

680 S3 Fig. Eggs laid in *O. fasciatus* ds-*dnmt1* and control females. (A) Number of eggs
681 laid by ds-*dnmt1* and control females 8-days post-injection. Dots indicate mean
682 expression level, and error bars indicate standard error of the mean.

683

## 684 S4 Fig. mCG in A. mellifera and Z. nevadensis is not associated with transcription.

(A) Gene expression level for deciles of increasing mCG (1–10) and un-methylated genes

686 (UM). Error bars represent 95% confidence interval of the mean. (B) Regression of gene

687 expression against a continuous measure of mCG among all genes with >0 FPKM and

688 weighted mCG. Raw p values are provided for each regression, and significance (S) or

689 non-significance (NS) is indicated in brackets following Bonferroni correction.

690

## 691 S5 Fig. Loss of mCG in *O. fasciatus* ovaries has a limited effect on transcription. (A)

692 Combinational overlap of genes that are differential CG-methylated and expressed, and

693 similarly CG-methylated and expressed between *O. fasciatus* ds-*dnmt1* and control. Gene

694 groups: Differentially Methylated Gene (DMG), Differentially Expressed Gene (DEG),

695 Similarly Methylated Gene (SMG)/UnMethylated Genes (UMG), and non-Differentially

696 Expressed Gene (non-DEG). More stringent thresholds were used to group genes as CG-

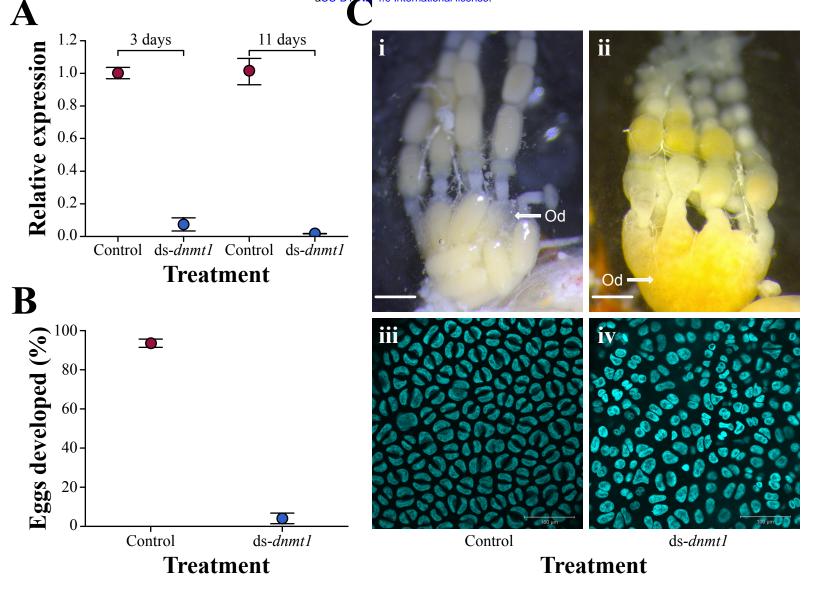
697 methylated or unmethylated (see Materials and Methods).

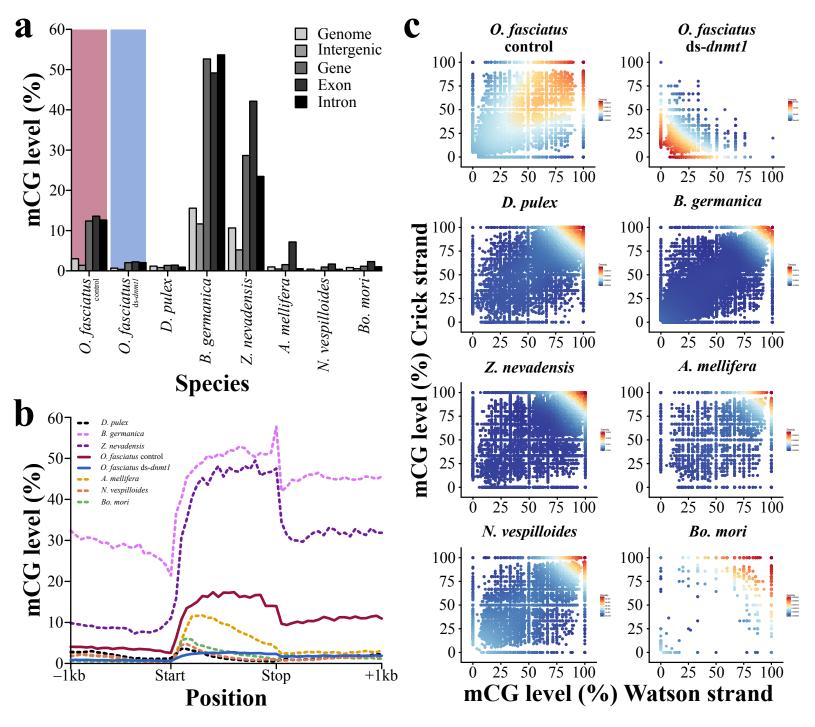
698

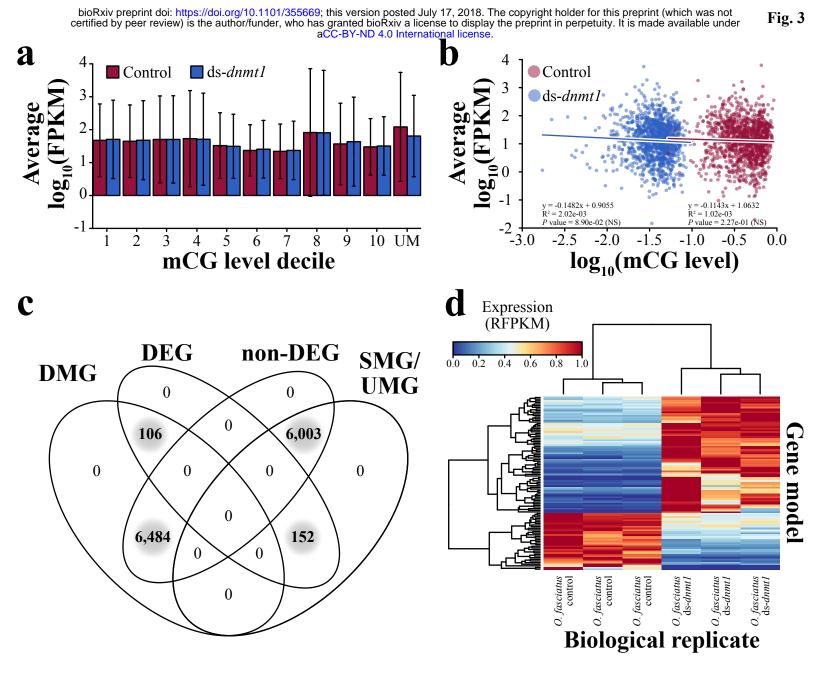
699 S6 Fig. DNA methylation of TEs in *O. fasciatus*. (A) Levels of mCG across the bodies
700 and 1kb flanking sequence of different annotated TEs in *O. fasciatus*.

702	S1 Table. PCR primers used to validate the presence of a single Dnmt1 ortholog in
703	the O. fasciatus genome.
704	
705	S2 Table. Primer sequences for use in producing template DNA for use in the
706	MegaScript transcription kit to generate double stranded RNAs for injection and
707	for quantitative real-time PCR to assess expression levels of Dnmt1.
708	
709	S3 Table. Overlap between O. fasciatus (control) CG-methylated and unmethylated
710	genes in none and $\geq$ 1 other insect species used in this study.
711	
712	S4 Table. DNA methylation summary statistics for all species investigated in this
713	study.
714	
715	S5 Table. Output from edgeR v3.20.1 [53] with gene expression (Fragments Per
716	Kilobase of transcript per Million mapped reads [FPKM]) for O. fasciatus ovaries
717	ds-dnmt1 and control biological and technical replicates.
718	
719	S6 Table. Gene expression FPKM for A. mellifera queen and drone brains.
720	
721	S7 Table. Gene expression (FPKM) for Z. nevadensis female worker at the final
722	instar larva.

724	S8 Table. Output from edgeR v3.20.1 [53] with gene expression (FPKM) for O.
725	fasciatus gut, head, and thorax ds-dnmt1 and control biological replicates.
726	
727	S9 Table. Output General Features File (GFF) from RepeatMasker v4.0.5
728	( <u>http://www.repeatmasker.org</u> ).
729	
730	S10 Table. Significance (p value) of TE expression between ds-dnmt1 and control
731	tissues.
732	
733	S11 Table. Gene Ontology (GO) terms for O. fasciatus v1.1 reference genome
734	assembly [26] annotated genes.
735	
736	S12 Table. Significantly enriched GO terms for the intersections between
737	Differentially Methylated Genes (DMG), Similarly Methylated Genes (SMG),
738	Differentially Expressed Genes (DEG), and non-Differentially Expressed Genes
739	(non-DEG).
740	
741	S1 Data. Unaligned and aligned DNA methyltransferase protein sequences in fasta
742	format, and a parenthetical phylogenetic tree in nexus format estimated from the
743	aligned DNA methyltransferase protein sequences using BEAST v2.3.2 [35].







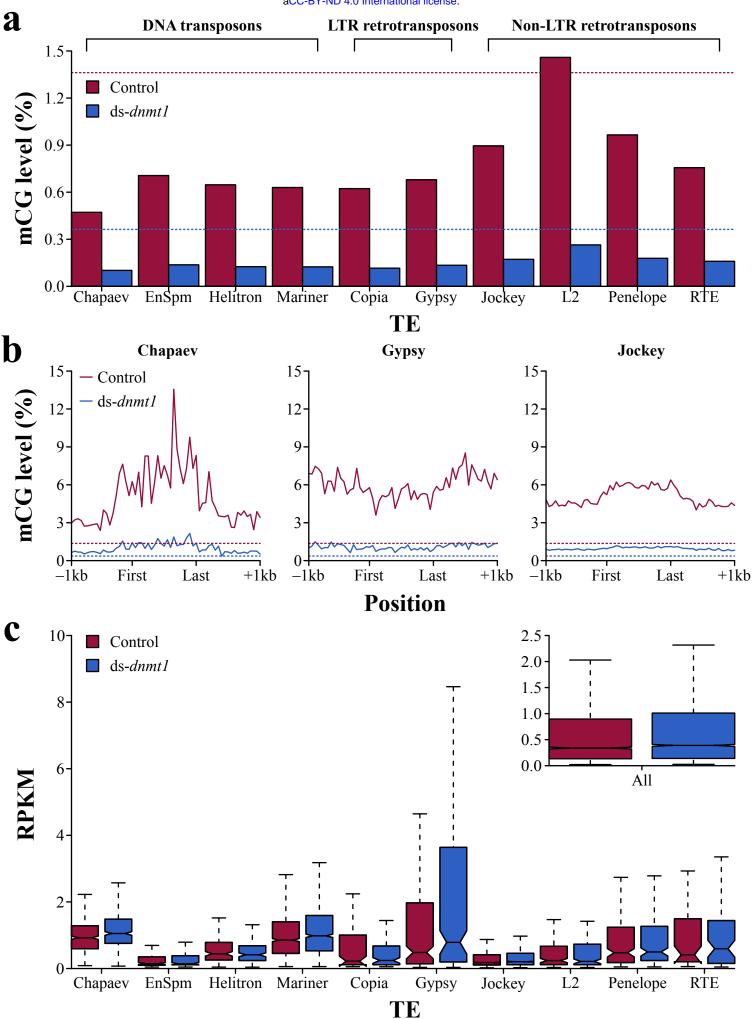


Fig. 4